(Preprint) AAS 26-796

SPACECRAFT BACKSUBSTITUTION DYNAMICS FOR GENERALIZED RIGID BODY COMPONENT MOTION

Leah Kiner* and Hanspeter Schaub†

The backsubstitution method is a modular spacecraft dynamics formulation which has been introduced to enable rapid software configuration and efficient execution of complex spacecraft simulations. The method was originally applied to model specific spacecraft subsystems including hinged panels, reaction wheels, fuel slosh, thrusters, and prescribed components. While recent work has focused on developing more generalized formulations capable of simulating a range of dynamically similar spacecraft components such as sequentially connected rotating or translating appendages, no fundamental formulation has been introduced to model rigid body component motion with complete generality. This work develops a new generalized backsubstitution formulation by considering the rigid spacecraft subcomponent as a general six degree-of-freedom joint. The results enable any type of rigid body component motion to be simulated under a single unified formulation. A multibody deployment numerical example illustrates the applicability and effectiveness of this modeling approach.

INTRODUCTION

Simulation of spacecraft dynamics is a fundamental part of the spacecraft mission design process. Especially as spacecraft systems continue to evolve, containing attached appendages with ever-increasing complexity, it is critical that the dynamics of these systems can be accurately modeled and simulated efficiently in software. The dynamics of rigid body systems are typically derived using a variety of different methods including Newtonian and Eulerian mechanics, Lagrangian mechanics, or Kane's method.[1,2] From there, the system equations of motion are typically first reorganized and afterward implemented in software with a chosen numerical integrator. The ease with which spacecraft simulations can be set up and reconfigured is an essential consideration which can have a profound impact on the long-term efficiency of the mission design process. Even simple changes to the initial spacecraft design can require tedious rederivations of the spacecraft system's equations of motion. This unfavorable process can be avoided through a judicious choice of the formulation used for the software implementation of the system equations. The benefits of a modular, scalable, and numerically efficient spacecraft dynamics formulation cannot be overstated. For these reasons, the field of multi-body spacecraft dynamics has been deeply studied for many decades.[3–14]

To solve the inverse dynamics problem of computing the joint forces required to produce given active joint velocities and accelerations, Luh et al. coined the $\mathcal{O}(n)$ recursive Newton-Euler method.[8]

*Graduate Research Assistant, Ann and H.J. Smead Department of Aerospace Engineering Sciences, University of Colorado Boulder, Colorado Center For Astrodynamics Research, Boulder, CO, 80303 USA. leah.kiner@colorado.edu

†Distinguished Professor, Glenn L. Murphy Endowed Chair, Ann and H.J. Smead Department of Aerospace Engineering Sciences, University of Colorado, Boulder, 431 UCB, Colorado Center for Astrodynamics Research, Boulder, CO, 80309. AAS Fellow, AIAA Fellow.

Walker and Orin first introduced the $\mathcal{O}(n^2)$ composite-rigid-body algorithm (CRBA) to compute the mass matrix for a kinematic tree, which was later improved and modified to be more efficient.[9,15] Featherstone later introduced a six-dimensional vector notation called spatial notation, where the linear and angular components of the rigid body motion are combined to yield a unified set of equations.[15–17] This approach greatly reduces the size and number of equations required to facilitate dynamics analysis and has been shown to significantly improve computational efficiency through recursive relations.[18] Improving the $\mathcal{O}(n^2)$ CRBA, Featherstone developed the $\mathcal{O}(n)$ forward dynamics articulated-body algorithm (ABA) which has been used in many robotics applications.[17] Spatial Operator Algebra (SOA) is a similar, widely applied dynamics formulation capable of simulating flexible multi-body systems efficiently in software using a reformulated spatial vector notation.[19–21] Used in the Jet Propulsion Laboratory's Dynamics Algorithms for Real-Time Simulation (DARTS) [*] software package, the method leverages linear operators acting on spatial vectors to derive more general recursive solutions. NASA's open-source software package 42 [†] utilizes a tree-topology approach for implementation of the spacecraft dynamics, which reduces the size of the system mass matrix for numerical integration.[3,5]

While the aforementioned formulations have been used extensively for many spacecraft dynamics applications, the backsubstitution method (BSM) is another dynamics formulation which has been gaining popularity in recent years due to its prioritization of software modularity, ease of setting up complex spacecraft dynamics simulations, scalability of the spacecraft model complexity, testability, and numerical efficiency.[22–25] By assuming all spacecraft components (effectors) such as solar panels, thrusters, or reaction wheels are attached to a central rigid hub structure, the resulting N component equations of motion are decoupled from one another in the system mass matrix and can be analytically back-substituted into the six hub equations of motion. This process reduces the dimension of the system mass matrix that must be inverted from 6 + N to 6. Schur decomposition further reduces the 6×6 matrix inversion to only two 3×3 inversions.[22,24] The decoupling of the component equations of motion facilitates a modular software implementation of the component-specific dynamics and a seamless testing and verification procedure for each component type. This modularity enables simulations to be rapidly scaled to any number of component attachments to the base hub structure without requiring any rederivation of the system equations of motion.[22]

The backsubstitution formulation has been applied to a wide variety of rigid body spacecraft systems. The method was first applied to specific component types including single and multi-hinged solar panels,[26] reaction wheels,[27] control moment gyroscopes,[28] fuel slosh,[29,30] and prescribed motion components.[31,32] Recent work has focused on expanding the original method to allow for component branching,[33–35] which has enabled select component-on-component attachments. Most relevant to this work, recent research efforts have also focused on generalizing the original method for more primitive component motions including chains of sequentially rotating or translating rigid bodies.[36–38] The results can be used to simulate a variety of dynamically similar components such as reaction wheels, robotic arms, or a multi-hinged and multi-modal solar panels. While these new formulations are incredibly versatile, they are limited to chains of identical joint types. Rotational and translational motion cannot be mixed. Addressing this limitation, this paper introduces a new backsubstitution formulation capable of simulating any type of rigid body component motion with absolute generality. The formulation assumes a rigid component with six general sequential degrees of freedom. The degrees of freedom may be configured in any order, where the user may choose

[*] `https://dartslab.jpl.nasa.gov/DARTS/index.php`
[†] `https://software.nasa.gov/software/GSC-16720-1`

from rotation, translation, or coupled screw motion. The resulting formulation is completely general and tremendously diverse, superseding prior developments of the backsubstitution method. The results are the first to permit full six degree-of-freedom, unconstrained rigid body motion, where any combination of serial-chain rigid body joint motion can be configured. For example, consider a component performing a helical screw-type deployment. While this is a one degree-of-freedom deployment, the component translational and rotational motion are coupled. The joint mapping formulation introduced in this work enables component motion to be simulated where multiple degrees of freedom are coupled.

This paper is organized as follows. First, the system problem statement is outlined which includes all component and frame definitions. Next, the rigid body joint notation is introduced and the joint kinematics are developed which are used in the equation of motion development. The following two sections develop the system and general component equations of motion using Newtonian and Eulerian mechanics. The developed equations are next organized into the form of the backsubstitution method, which is the form chosen for the dynamics software implementation. A multi-body numerical deployment scenario illustrating the applicability of the derived results is next presented, followed by the concluding remarks.

PROBLEM STATEMENT

Figure (1) illustrates the general system of interest for the derivation in this work. The system includes a six degree-of-freedom rigid hub (gray) and a general six-degree-of-freedom rigid component (orange). Note that while only a single general component is shown attached to the hub structure, the derivation results are immediately scalable to N general component attachments to the hub.

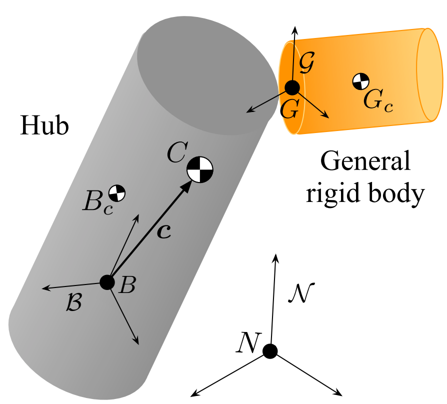

Figure 1. Problem statement for the general system.

Three reference frames are required to derive system dynamics. First, an inertial frame indicated by $\mathcal{N} : \{N, \hat{\boldsymbol{n}}_1, \hat{\boldsymbol{n}}_2, \hat{\boldsymbol{n}}_3\}$ is used as the base of reference for the dynamics. The motion of the rigid hub is described using the frame $\mathcal{B} : \{B, \hat{\boldsymbol{b}}_1, \hat{\boldsymbol{b}}_2, \hat{\boldsymbol{b}}_3\}$, while the motion of the general component is defined using the joint frame $\mathcal{G} : \{G, \hat{\boldsymbol{g}}_1, \hat{\boldsymbol{g}}_2, \hat{\boldsymbol{g}}_3\}$. The origin points of these frames are given by N, B and G, respectively. The masses of the system bodies are defined as m_{hub} and m_{G}. Finally, the center of mass points of each body are indicated by B_c and G_c.

JOINT KINEMATICS

The kinematics of the general component illustrated in Fig. 1 can be fully defined using its joint frame $\mathcal{G}$, a general degree-of-freedom matrix $\boldsymbol{\beta}$ of size $N \times 1$, and mapping vectrix (matrix of vectors) $[\boldsymbol{T}]$ of size $6 \times N$. The variable $N \leq 6$ indicates the total number of degrees of freedom of the general component. Each degree of freedom is applied sequentially in the order indicated by the matrix $\boldsymbol{\beta}$.

The mapping vectrix is used to map the general component scalar degrees of freedom to its hub-relative translational and rotational vector states. The translational and rotational axes associated with each degree of freedom are stored in the upper and lower halves of the mapping vectrix, respectively. For example, a rigid body modeled as a 1 degree-of-freedom revolute joint has the mapping vectrix $[\boldsymbol{T}] = \begin{bmatrix} \mathbf{0}_{3\times1} \\ \hat{\boldsymbol{g}}_\theta \end{bmatrix}$ and degree-of-freedom matrix $\boldsymbol{\beta} = [\theta]$. Table (1) provides several simple joint types and their corresponding joint parameters.

Joint Type	N	$[\boldsymbol{T}]$	$\boldsymbol{\beta}$
Revolute	1	$\begin{bmatrix} \mathbf{0} \\ \hat{\boldsymbol{g}}_\theta \end{bmatrix}$	$[\theta]$
Prismatic	1	$\begin{bmatrix} \hat{\boldsymbol{g}}_\rho \\ \mathbf{0} \end{bmatrix}$	$[\rho]$
Helical Screw	1	$\begin{bmatrix} c\hat{\boldsymbol{g}}_\theta \\ \hat{\boldsymbol{g}}_\theta \end{bmatrix}$	$[\theta]$
Cylindrical	2	$\begin{bmatrix} \hat{\boldsymbol{g}}_\rho & \mathbf{0} \\ \mathbf{0} & \hat{\boldsymbol{g}}_\theta \end{bmatrix}$	$\begin{bmatrix} \rho \\ \theta \end{bmatrix}$

Table 1. Joint types.

Through definition of $[\Phi_\rho] = \begin{bmatrix} [I]_{3\times3} & [\mathbf{0}]_{3\times3} \end{bmatrix}$ and $[\Phi_\theta] = \begin{bmatrix} [\mathbf{0}]_{3\times3} & [I]_{3\times3} \end{bmatrix}$, the general body displacement and angular velocity relative to the hub are defined as

$$\boldsymbol{r}_{G/B} = [\Phi_\rho][\boldsymbol{T}]\boldsymbol{\beta} \tag{1}$$

$$\boldsymbol{\omega}_{\mathcal{G}/\mathcal{B}} = [\Phi_\theta][\boldsymbol{T}]\dot{\boldsymbol{\beta}} \tag{2}$$

Next, hub-relative time derivatives (indicated with a right superscript $'$) of Eqs. (1) and (2) are taken, yielding the general body velocity and acceleration kinematics

$$\boldsymbol{r}'_{G/B} = [\Phi_\rho]\left([\boldsymbol{T}']\boldsymbol{\beta} + [\boldsymbol{T}]\dot{\boldsymbol{\beta}}\right) \tag{3}$$

$$\boldsymbol{r}''_{G/B} = [\Phi_\rho]\left([\boldsymbol{T}'']\boldsymbol{\beta} + 2[\boldsymbol{T}']\dot{\boldsymbol{\beta}} + [\boldsymbol{T}]\ddot{\boldsymbol{\beta}}\right) \tag{4}$$

$$\boldsymbol{\omega}'_{\mathcal{G}/\mathcal{B}} = [\Phi_\theta][\boldsymbol{T}]\ddot{\boldsymbol{\beta}} + [\Phi_\theta][\boldsymbol{T}']\dot{\boldsymbol{\beta}} \tag{5}$$

Note that the term $[\boldsymbol{T}'']$ contains additional terms coupled with the general body scalar acceleration matrix $\ddot{\boldsymbol{\beta}}$ and must be expanded. First, the joint mapping vectrix and its hub-relative time derivatives are defined as

$$[\boldsymbol{T}] = \begin{bmatrix} \boldsymbol{t}_1 & \cdots & \boldsymbol{t}_i & \cdots & \boldsymbol{t}_N \end{bmatrix} \tag{6}$$

$$[\boldsymbol{T}'] = \begin{bmatrix} \boldsymbol{t}'_1 & \cdots & \boldsymbol{t}'_i & \cdots & \boldsymbol{t}'_N \end{bmatrix} \tag{7}$$

$$[\boldsymbol{T}''] = \begin{bmatrix} \boldsymbol{t}''_1 & \cdots & \boldsymbol{t}''_i & \cdots & \boldsymbol{t}''_N \end{bmatrix} \tag{8}$$

where

$$\boldsymbol{t}'_i = \begin{bmatrix} \left[\widetilde{\boldsymbol{\omega}_{\mathcal{G}_{i-1}/\mathcal{B}}}\right] & [\mathbf{0}] \\ [\mathbf{0}] & \left[\widetilde{\boldsymbol{\omega}_{\mathcal{G}_{i-1}/\mathcal{B}}}\right] \end{bmatrix} \boldsymbol{t}_i = \underbrace{\left[\widetilde{\boldsymbol{\omega}_{\mathcal{G}_{i-1}/\mathcal{B}}}\right]}_{6\times 6} \boldsymbol{t}_i \tag{9}$$

$$\begin{aligned} \boldsymbol{t}''_i &= \begin{bmatrix} \left[\widetilde{\boldsymbol{\omega}'_{\mathcal{G}_{i-1}/\mathcal{B}}}\right] + \left[\widetilde{\boldsymbol{\omega}_{\mathcal{G}_{i-1}/\mathcal{B}}}\right]^2 & [\mathbf{0}] \\ [\mathbf{0}] & \left[\widetilde{\boldsymbol{\omega}'_{\mathcal{G}_{i-1}/\mathcal{B}}}\right] + \left[\widetilde{\boldsymbol{\omega}_{\mathcal{G}_{i-1}/\mathcal{B}}}\right]^2 \end{bmatrix} \boldsymbol{t}_i \\ &= \left(\underbrace{\left[\widetilde{\boldsymbol{\omega}'_{\mathcal{G}_{i-1}/\mathcal{B}}}\right]}_{6\times 6} + \underbrace{\left[\widetilde{\boldsymbol{\omega}_{\mathcal{G}_{i-1}/\mathcal{B}}}\right]^2}_{6\times 6} \right) \boldsymbol{t}_i \end{aligned} \tag{10}$$

The tilde matrix indicates the cross product operator: $\boldsymbol{v} \times \boldsymbol{w} = [\tilde{\boldsymbol{v}}]\boldsymbol{w}$ where $[\tilde{\boldsymbol{v}}]$ is a 3×3 skew-symmetric matrix and the components of $\boldsymbol{v}$ and $\boldsymbol{w}$ are expressed in the same frame.[2]

The angular velocity and angular acceleration of the ith degree of freedom are

$$\boldsymbol{\omega}_{\mathcal{G}_i/\mathcal{B}} = [\Phi_\theta] \sum_{j=1}^{i} \dot{\beta}_j \boldsymbol{t}_j \tag{11}$$

$$\boldsymbol{\omega}'_{\mathcal{G}_i/\mathcal{B}} = [\Phi_\theta] \sum_{j=1}^{i} \left(\dot{\beta}_j \boldsymbol{t}'_j + \ddot{\beta}_j \boldsymbol{t}_j \right) = [\Phi_\theta] \sum_{j=1}^{i} \left(\dot{\beta}_j \underbrace{\left[\widetilde{\boldsymbol{\omega}_{\mathcal{G}_{j-1}/\mathcal{B}}}\right]}_{6\times 6} + \ddot{\beta}_j \right) \boldsymbol{t}_j \tag{12}$$

Substitution of Eq. (12) into Eq. (10) and separating terms for clarity yields the result

$$\begin{aligned} \boldsymbol{t}''_i &= \left(\underbrace{\left[\widetilde{[\Phi_\theta] \sum_{j=1}^{i-1} \left(\dot{\beta}_j \underbrace{\left[\widetilde{\boldsymbol{\omega}_{\mathcal{G}_{j-1}/\mathcal{B}}}\right]}_{6\times 6} + \ddot{\beta}_j \right) \boldsymbol{t}_j} \right]}_{6\times 6} + \underbrace{\left[\widetilde{\boldsymbol{\omega}_{\mathcal{G}_{i-1}/\mathcal{B}}}\right]^2}_{6\times 6} \right) \boldsymbol{t}_i \\ &= \underbrace{\left[\widetilde{[\Phi_\theta] \sum_{j=1}^{i-1} \dot{\beta}_j \underbrace{\left[\widetilde{\boldsymbol{\omega}_{\mathcal{G}_{j-1}/\mathcal{B}}}\right]}_{6\times 6} \boldsymbol{t}_j} \right]}_{6\times 6} \boldsymbol{t}_i + \underbrace{\left[\widetilde{[\Phi_\theta] \sum_{j=1}^{i-1} \ddot{\beta}_j \boldsymbol{t}_j} \right]}_{6\times 6} \boldsymbol{t}_i + \underbrace{\left[\widetilde{\boldsymbol{\omega}_{\mathcal{G}_{i-1}/\mathcal{B}}}\right]^2}_{6\times 6} \boldsymbol{t}_i \end{aligned} \tag{13}$$

To reduce Eq. (4) further, next we specifically examine $[\boldsymbol{T}'']\boldsymbol{\beta}$ in more detail:

$$[\boldsymbol{T}'']\boldsymbol{\beta} = \sum_{i=1}^{N} \beta_i \boldsymbol{t}_i'' \tag{14}$$

Substitution of Eq. (13) into Eq. (14) gives

$$[\boldsymbol{T}'']\boldsymbol{\beta} = \sum_{i=1}^{N} \beta_i \underbrace{\left[[\Phi_\theta] \widetilde{\sum_{j=1}^{i-1} \ddot{\beta}_j \boldsymbol{t}_j} \right]}_{6\times 6} \boldsymbol{t}_i + \sum_{i=1}^{N} \beta_i \underbrace{\left[[\Phi_\theta] \widetilde{\sum_{j=1}^{i-1} \dot{\beta}_j \underbrace{\left[\widetilde{\boldsymbol{\omega}_{\mathcal{G}_{j-1}/\mathcal{B}}} \right]}_{6\times 6} \boldsymbol{t}_j} \right]}_{6\times 6} \boldsymbol{t}_i + \sum_{i=1}^{N} \beta_i \underbrace{\left[\widetilde{\boldsymbol{\omega}_{\mathcal{G}_{i-1}/\mathcal{B}}} \right]^2}_{6\times 6} \boldsymbol{t}_i \tag{15}$$

To be used in the backsubstitution formulation, we next seek a form of $[\boldsymbol{T}'']\boldsymbol{\beta} = [\boldsymbol{U}]\ddot{\boldsymbol{\beta}} + \boldsymbol{v}$ for the kinematics. All terms coupled with the general body scalar accelerations are collected in the matrix $[\boldsymbol{U}]$. Terms not coupled with $\ddot{\boldsymbol{\beta}}$ are collected in the vector $\boldsymbol{v}$, where clearly

$$\boldsymbol{v} = \sum_{i=1}^{N} \beta_i \underbrace{\left[[\Phi_\theta] \widetilde{\sum_{j=1}^{i-1} \dot{\beta}_j \underbrace{\left[\widetilde{\boldsymbol{\omega}_{\mathcal{G}_{j-1}/\mathcal{B}}} \right]}_{6\times 6} \boldsymbol{t}_j} \right]}_{6\times 6} \boldsymbol{t}_i + \sum_{i=1}^{N} \beta_i \underbrace{\left[\widetilde{\boldsymbol{\omega}_{\mathcal{G}_{i-1}/\mathcal{B}}} \right]^2}_{6\times 6} \boldsymbol{t}_i \tag{16}$$

Manipulating the summations in the remaining $[\boldsymbol{T}'']\boldsymbol{\beta}$ terms coupled with $\ddot{\boldsymbol{\beta}}$ yields the desired result

$$[\boldsymbol{U}] = \left[\underbrace{\left[\widetilde{[\Phi_\theta]\boldsymbol{t}_1} \right]}_{6\times 6} \textstyle\sum_{i=2}^{N} \beta_i \boldsymbol{t}_i \quad \underbrace{\left[\widetilde{[\Phi_\theta]\boldsymbol{t}_2} \right]}_{6\times 6} \textstyle\sum_{i=3}^{N} \beta_i \boldsymbol{t}_i \quad \underbrace{\left[\widetilde{[\Phi_\theta]\boldsymbol{t}_3} \right]}_{6\times 6} \textstyle\sum_{i=4}^{N} \beta_i \boldsymbol{t}_i \quad \cdots \quad \underbrace{\boldsymbol{0}}_{6\times 1} \right] \tag{17}$$

Finally, substitution of $[\boldsymbol{T}'']\boldsymbol{\beta} = [\boldsymbol{U}]\ddot{\boldsymbol{\beta}} + \boldsymbol{v}$ into Eq. (4) yields the desired form for the general body hub-relative translational acceleration

$$\boldsymbol{r}''_{G/B} = [\Phi_\rho] \left([\boldsymbol{T}] + [\boldsymbol{U}] \right) \ddot{\boldsymbol{\beta}} + [\Phi_\rho] \left(2[\boldsymbol{T}']\dot{\boldsymbol{\beta}} + \boldsymbol{v} \right) \tag{18}$$

The final step in the kinematics development is resolving the general body center of mass kinematics

$$\boldsymbol{r}_{G_c/B} = \boldsymbol{r}_{G_c/G} + \boldsymbol{r}_{G/B} \tag{19}$$

$$\boldsymbol{r}'_{G_c/B} = [\tilde{\boldsymbol{\omega}}_{\mathcal{G}/\mathcal{B}}]\boldsymbol{r}_{G_c/G} + \boldsymbol{r}'_{G/B} \tag{20}$$

$$\boldsymbol{r}''_{G_c/B} = \left([\tilde{\boldsymbol{\omega}}'_{\mathcal{G}/\mathcal{B}}] + [\tilde{\boldsymbol{\omega}}_{\mathcal{G}/\mathcal{B}}]^2 \right) \boldsymbol{r}_{G_c/G} + \boldsymbol{r}''_{G/B} \tag{21}$$

Substitution of Eqs. (1-5) and (18) into the above equations gives the general body center of mass kinematics

$$\boldsymbol{r}_{G_c/B} = \boldsymbol{r}_{G_c/G} + [\Phi_\rho][\boldsymbol{T}]\boldsymbol{\beta} \tag{22}$$

$$\boldsymbol{r}'_{G_c/B} = \left[\widetilde{[\Phi_\theta][\boldsymbol{T}]\dot{\boldsymbol{\beta}}}\right]\boldsymbol{r}_{G_c/G} + [\Phi_\rho]\left([\boldsymbol{T}']\boldsymbol{\beta} + [\boldsymbol{T}]\dot{\boldsymbol{\beta}}\right) \tag{23}$$

$$\begin{aligned}\boldsymbol{r}''_{G_c/B} &= \left(\left([\Phi_\rho] - \left[\tilde{\boldsymbol{r}}_{G_c/G}\right][\Phi_\theta]\right)[\boldsymbol{T}] + [\Phi_\rho][\boldsymbol{U}]\right)\ddot{\boldsymbol{\beta}} \\ &\quad + \left(2[\Phi_\rho] - \left[\tilde{\boldsymbol{r}}_{G_c/G}\right][\Phi_\theta]\right)[\boldsymbol{T}']\dot{\boldsymbol{\beta}} \\ &\quad + \left[\widetilde{[\Phi_\theta][\boldsymbol{T}]\dot{\boldsymbol{\beta}}}\right]^2\boldsymbol{r}_{G_c/G} + [\Phi_\rho]\boldsymbol{v}\end{aligned} \tag{24}$$

EQUATIONS OF MOTION DERIVATION

This section derives the general equations of motion for the general rigid body system shown in Fig. (1). Newtonian and Eulerian mechanics are used for the equation-of-motion development. Note that that while the derivation considers only a single general body, the results are immediately scalable for N single-body attachments to the spacecraft hub.

System Translational Equations of Motion

The spacecraft hub translational equations of motion define the first three system degrees of freedom. These equations are derived starting from Newton's Second Law for the spacecraft center of mass[2]

$$m_{\text{sc}}\ddot{\boldsymbol{r}}_{C/N} = m_{\text{sc}}\ddot{\boldsymbol{c}} + m_{\text{sc}}\ddot{\boldsymbol{r}}_{B/N} = \sum \boldsymbol{F}_{\text{ext}} \tag{25}$$

where m_{sc} is the total mass of the spacecraft system, $m_{\text{sc}} = m_{\text{hub}} + m_{\text{G}}$, and $\sum \boldsymbol{F}_{\text{ext}}$ is the sum of all external forces acting on the system. Note that because the hub equations of motion are of interest for this formulation, the acceleration of the hub frame origin point B must be defined. First, the transport theorem[2] is used to relate the hub-relative derivative of the center of mass vector to its inertial time derivative

$$\dot{\boldsymbol{c}} = \boldsymbol{c}' + \boldsymbol{\omega}_{\mathcal{B}/\mathcal{N}} \times \boldsymbol{c} \tag{26}$$

$$\ddot{\boldsymbol{c}} = \boldsymbol{c}'' + 2\boldsymbol{\omega}_{\mathcal{B}/\mathcal{N}} \times \boldsymbol{c}' + \dot{\boldsymbol{\omega}}_{\mathcal{B}/\mathcal{N}} \times \boldsymbol{c} + \boldsymbol{\omega}_{\mathcal{B}/\mathcal{N}} \times \boldsymbol{\omega}_{\mathcal{B}/\mathcal{N}} \times \boldsymbol{c} \tag{27}$$

The system center of mass vector is defined using the mass contributions from all of the system bodies

$$\boldsymbol{c} = \frac{m_{\text{hub}}\boldsymbol{r}_{B_c/B} + m_{\text{G}}\boldsymbol{r}_{G_c/B}}{m_{\text{sc}}} \tag{28}$$

The hub-relative velocity of the center of mass vector is

$$\boldsymbol{c}' = \frac{m_{\text{G}}\boldsymbol{r}'_{G_c/B}}{m_{\text{sc}}} \tag{29}$$

Similarly, the hub-relative acceleration of the center of mass vector is

$$\boldsymbol{c}'' = \frac{m_{\text{G}}\boldsymbol{r}''_{G_c/B}}{m_{\text{sc}}} \tag{30}$$

Substituting Eqs. (27) and (30) into Eq. (25) yields a compact expression for the system translational equations of motion

$$m_{\text{sc}}\ddot{\boldsymbol{r}}_{B/N} + m_{\text{sc}}[\dot{\tilde{\boldsymbol{\omega}}}_{\mathcal{B}/\mathcal{N}}]\boldsymbol{c} = \sum \boldsymbol{F}_{\text{ext}} - 2m_{\text{sc}}[\tilde{\boldsymbol{\omega}}_{\mathcal{B}/\mathcal{N}}]\boldsymbol{c}' - m_{\text{sc}}[\tilde{\boldsymbol{\omega}}_{\mathcal{B}/\mathcal{N}}]^2\boldsymbol{c} - m_{\text{G}}\boldsymbol{r}''_{G_c/B} \tag{31}$$

The final step required to obtain the final form for the hub translational equations of motion is substitution Eq. (24) into Eq. (31)

$$
\begin{aligned}
m_{\text{sc}}\ddot{\boldsymbol{r}}_{B/N} + m_{\text{sc}}[\dot{\tilde{\boldsymbol{\omega}}}_{\mathcal{B}/\mathcal{N}}]\boldsymbol{c} + m_{\text{G}}\left(\left([\Phi_\rho] - \left[\tilde{\boldsymbol{r}}_{G_c/G}\right][\Phi_\theta]\right)[\boldsymbol{T}] + [\Phi_\rho][\boldsymbol{U}]\right)\ddot{\boldsymbol{\beta}} = \sum \boldsymbol{F}_{\text{ext}} \\
- 2m_{\text{sc}}[\tilde{\boldsymbol{\omega}}_{\mathcal{B}/\mathcal{N}}]\boldsymbol{c}' - m_{\text{sc}}[\tilde{\boldsymbol{\omega}}_{\mathcal{B}/\mathcal{N}}]^2\boldsymbol{c} - m_{\text{G}}\left(2[\Phi_\rho] - \left[\tilde{\boldsymbol{r}}_{G_c/G}\right][\Phi_\theta]\right)[\boldsymbol{T}']\dot{\boldsymbol{\beta}} \\
- m_{\text{G}}\left[\widetilde{[\Phi_\theta][\boldsymbol{T}]\dot{\boldsymbol{\beta}}}\right]^2\boldsymbol{r}_{G_c/G} - m_{\text{G}}[\Phi_\rho]\boldsymbol{v}
\end{aligned} \tag{32}
$$

System Rotational Equations of Motion

The spacecraft hub rotational equations of motion describe the three remaining hub degrees of freedom. The derivation begins by applying Euler's equation to the case where the spacecraft angular momentum is expressed about a hub-fixed point not coincident with the system center of mass[2]

$$
\dot{\boldsymbol{H}}_{\text{sc},B} = \sum \boldsymbol{L}_B + m_{\text{sc}}\ddot{\boldsymbol{r}}_{B/N} \times \boldsymbol{c} \tag{33}
$$

where $\boldsymbol{H}_{\text{sc},B}$ is the inertial angular momentum of the spacecraft system about point B and $\sum \boldsymbol{L}_B$ is the total external torque acting on the system about point B. First, the system angular momentum about point B is

$$
\begin{aligned}
\boldsymbol{H}_{\text{sc},B} = \boldsymbol{H}_{\text{hub},B} + \boldsymbol{H}_{\text{G},B} = ([I_{\text{hub},B}] + [I_{\text{G},B}])\,\boldsymbol{\omega}_{\mathcal{B}/\mathcal{N}} \\
+ [I_{\text{G},G_c}]\boldsymbol{\omega}_{\mathcal{G}/\mathcal{B}} + m_{\text{G}}[\tilde{\boldsymbol{r}}_{G_c/B}]\boldsymbol{r}'_{G_c/B}
\end{aligned} \tag{34}
$$

where $[I_{\text{hub},B}]$ and $[I_{\text{G},B}]$ are the hub and general body inertia tensors about point B. $[I_{\text{G},G_c}]$ is the general body inertia tensor about its center of mass. Combining both inertia tensors about point B yields the total spacecraft inertia about point B

$$
[I_{\text{sc},B}] = [I_{\text{hub},B}] + [I_{\text{G},B}] \tag{35}
$$

Simplifying reduces Eq. (34) to

$$
\boldsymbol{H}_{\text{sc},B} = [I_{\text{sc},B}]\boldsymbol{\omega}_{\mathcal{B}/\mathcal{N}} + [I_{\text{G},G_c}]\boldsymbol{\omega}_{\mathcal{G}/\mathcal{B}} + m_{\text{G}}[\tilde{\boldsymbol{r}}_{G_c/B}]\boldsymbol{r}'_{G_c/B} \tag{36}
$$

Next, the inertial time derivative of the total spacecraft angular momentum is expressed using the transport theorem as

$$
\begin{aligned}
\dot{\boldsymbol{H}}_{\text{sc},B} = [I'_{\text{sc},B}]\boldsymbol{\omega}_{\mathcal{B}/\mathcal{N}} + [I_{\text{sc},B}]\dot{\boldsymbol{\omega}}_{\mathcal{B}/\mathcal{N}} + [I_{\text{G},G_c}]\boldsymbol{\omega}'_{\mathcal{G}/\mathcal{B}} + [\tilde{\boldsymbol{\omega}}_{\mathcal{G}/\mathcal{N}}][I_{\text{G},G_c}]\boldsymbol{\omega}_{\mathcal{G}/\mathcal{B}} \\
+ m_{\text{G}}[\tilde{\boldsymbol{r}}_{G_c/B}]\boldsymbol{r}''_{G_c/B} + m_{\text{G}}[\tilde{\boldsymbol{\omega}}_{\mathcal{B}/\mathcal{N}}][\tilde{\boldsymbol{r}}_{G_c/B}]\boldsymbol{r}'_{G_c/B}
\end{aligned} \tag{37}
$$

Using the rigid body assumption for the hub and the parallel axis theorem to express the general body inertia about point B yields the $\mathcal{B}$ frame derivative of the spacecraft inertia tensor

$$
[I'_{\text{sc},B}] = [I'_{\text{G},B}] \ = [I'_{\text{G},G_c}] + m_{\text{G}}\left([\tilde{\boldsymbol{r}}'_{G_c/B}][\tilde{\boldsymbol{r}}_{G_c/B}]^T + [\tilde{\boldsymbol{r}}_{G_c/B}][\tilde{\boldsymbol{r}}'_{G_c/B}]^T\right) \tag{38}
$$

The inertia transport theorem[39] is used to express the general body inertia about its center of mass

$$
[I'_{\text{G},G_c}] = [\tilde{\boldsymbol{\omega}}_{\mathcal{G}/\mathcal{B}}][I_{\text{G},G_c}] - [I_{\text{G},G_c}][\tilde{\boldsymbol{\omega}}_{\mathcal{G}/\mathcal{B}}] \tag{39}
$$

Equation (38) then becomes

$$[I'_{\text{sc},B}] = [\tilde{\boldsymbol{\omega}}_{\mathcal{G}/\mathcal{B}}][I_{\text{G},G_c}] - [I_{\text{G},G_c}][\tilde{\boldsymbol{\omega}}_{\mathcal{G}/\mathcal{B}}] + m_{\text{G}}\left([\tilde{\boldsymbol{r}}'_{G_c/B}][\tilde{\boldsymbol{r}}_{G_c/B}]^T + [\tilde{\boldsymbol{r}}_{G_c/B}][\tilde{\boldsymbol{r}}'_{G_c/B}]^T\right) \tag{40}$$

Combining these results and arranging the terms in the form of the backsubstitution method yields the system rotational equations of motion

$$\begin{aligned} m_{\text{sc}}[\tilde{\boldsymbol{c}}]\ddot{\boldsymbol{r}}_{B/N} + [I_{\text{sc},B}]\dot{\boldsymbol{\omega}}_{\mathcal{B}/\mathcal{N}} &= \sum \boldsymbol{L}_B - \left([I'_{\text{sc},B}] + [\tilde{\boldsymbol{\omega}}_{\mathcal{B}/\mathcal{N}}][I_{\text{sc},B}]\right)\boldsymbol{\omega}_{\mathcal{B}/\mathcal{N}} \\ &- \left([I_{\text{G},G_c}]\boldsymbol{\omega}'_{\mathcal{G}/\mathcal{B}} + m_{\text{G}}[\tilde{\boldsymbol{r}}_{G_c/B}]\boldsymbol{r}''_{G_c/B} + [\tilde{\boldsymbol{\omega}}_{\mathcal{G}/\mathcal{N}}][I_{\text{G},G_c}]\boldsymbol{\omega}_{\mathcal{G}/\mathcal{B}} + m_{\text{G}}[\tilde{\boldsymbol{\omega}}_{\mathcal{B}/\mathcal{N}}][\tilde{\boldsymbol{r}}_{G_c/B}]\boldsymbol{r}'_{G_c/B}\right) \end{aligned} \tag{41}$$

Substitution of the joint kinematics into Eq. (41) gives the final form for the hub rotational equations of motion

$$\begin{aligned} & m_{\text{sc}}[\tilde{\boldsymbol{c}}]\ddot{\boldsymbol{r}}_{B/N} + [I_{\text{sc},B}]\dot{\boldsymbol{\omega}}_{\mathcal{B}/\mathcal{N}} \\ &\quad + \left([I_{\text{G},G_c}][\Phi_\theta][\boldsymbol{T}] + m_{\text{G}}\left[\widetilde{\boldsymbol{r}_{G_c/G} + [\Phi_\rho][\boldsymbol{T}]\boldsymbol{\beta}}\right]\left(\left([\Phi_\rho] - \left[\tilde{\boldsymbol{r}}_{G_c/G}\right][\Phi_\theta]\right)[\boldsymbol{T}] + [\Phi_\rho][\boldsymbol{U}]\right)\right)\ddot{\boldsymbol{\beta}} \\ &\quad = \sum \boldsymbol{L}_B - \left([I'_{\text{sc},B}] + [\tilde{\boldsymbol{\omega}}_{\mathcal{B}/\mathcal{N}}][I_{\text{sc},B}]\right)\boldsymbol{\omega}_{\mathcal{B}/\mathcal{N}} \\ &\quad - [I_{\text{G},G_c}][\Phi_\theta][\boldsymbol{T}']\dot{\boldsymbol{\beta}} - \left[\widetilde{[\Phi_\theta][\boldsymbol{T}]\dot{\boldsymbol{\beta}} + \boldsymbol{\omega}_{\mathcal{B}/\mathcal{N}}}\right][I_{\text{G},G_c}][\Phi_\theta][\boldsymbol{T}]\dot{\boldsymbol{\beta}} \\ &\quad - m_{\text{G}}\left[\widetilde{\boldsymbol{r}_{G_c/G} + [\Phi_\rho][\boldsymbol{T}]\boldsymbol{\beta}}\right]\left(\left(2[\Phi_\rho] - \left[\tilde{\boldsymbol{r}}_{G_c/G}\right][\Phi_\theta]\right)[\boldsymbol{T}']\dot{\boldsymbol{\beta}} + \left[\widetilde{[\Phi_\theta][\boldsymbol{T}]\dot{\boldsymbol{\beta}}}\right]^2\boldsymbol{r}_{G_c/G} + [\Phi_\rho]\boldsymbol{v}\right) \\ &\quad - m_{\text{G}}[\tilde{\boldsymbol{\omega}}_{\mathcal{B}/\mathcal{N}}]\left[\widetilde{\boldsymbol{r}_{G_c/G} + [\Phi_\rho][\boldsymbol{T}]\boldsymbol{\beta}}\right]\left(\left([\Phi_\rho] - \left[\tilde{\boldsymbol{r}}_{G_c/G}\right][\Phi_\theta]\right)[\boldsymbol{T}]\dot{\boldsymbol{\beta}} + [\Phi_\rho][\boldsymbol{T}']\boldsymbol{\beta}\right) \end{aligned} \tag{42}$$

General Body Translational Equations of Motion

The general body translational equations of motion are derived using Newton's second law

$$m_{\text{G}}\ddot{\boldsymbol{r}}_{G_c/N} = \sum \boldsymbol{F}_{\text{G}} \tag{43}$$

where

$$\ddot{\boldsymbol{r}}_{G_c/N} = \boldsymbol{r}''_{G_c/B} + 2[\tilde{\boldsymbol{\omega}}_{\mathcal{B}/\mathcal{N}}]\boldsymbol{r}'_{G_c/B} + \left([\dot{\tilde{\boldsymbol{\omega}}}_{\mathcal{B}/\mathcal{N}}] + [\tilde{\boldsymbol{\omega}}_{\mathcal{B}/\mathcal{N}}]^2\right)\boldsymbol{r}_{G_c/B} + \ddot{\boldsymbol{r}}_{B/N} \tag{44}$$

Substitution of the general body kinematics into Eq. (44), followed by substitution of Eq. (44) into Eq. (43) yields the general body translational equations of motion

$$\begin{aligned} & m_{\text{G}}\left(\left([\Phi_\rho] - \left[\tilde{\boldsymbol{r}}_{G_c/G}\right][\Phi_\theta]\right)[\boldsymbol{T}] + [\Phi_\rho][\boldsymbol{U}]\right)\ddot{\boldsymbol{\beta}} = -m_{\text{G}}\ddot{\boldsymbol{r}}_{B/N} + m_{\text{G}}\left[\widetilde{\boldsymbol{r}_{G_c/G} + [\Phi_\rho][\boldsymbol{T}]\boldsymbol{\beta}}\right]\dot{\boldsymbol{\omega}}_{\mathcal{B}/\mathcal{N}} \\ &\quad + \sum \boldsymbol{F}_{\text{G}} - 2m_{\text{G}}[\tilde{\boldsymbol{\omega}}_{\mathcal{B}/\mathcal{N}}]\left(\left([\Phi_\rho] - \left[\tilde{\boldsymbol{r}}_{G_c/G}\right][\Phi_\theta]\right)[\boldsymbol{T}]\dot{\boldsymbol{\beta}} + [\Phi_\rho][\boldsymbol{T}']\boldsymbol{\beta}\right) \\ &\quad - m_{\text{G}}[\tilde{\boldsymbol{\omega}}_{\mathcal{B}/\mathcal{N}}]^2\left(\boldsymbol{r}_{G_c/G} + [\Phi_\rho][\boldsymbol{T}]\boldsymbol{\beta}\right) - m_{\text{G}}\left(2[\Phi_\rho] - \left[\tilde{\boldsymbol{r}}_{G_c/G}\right][\Phi_\theta]\right)[\boldsymbol{T}']\dot{\boldsymbol{\beta}} \\ &\quad - m_{\text{G}}\left[\widetilde{[\Phi_\theta][\boldsymbol{T}]\dot{\boldsymbol{\beta}}}\right]^2\boldsymbol{r}_{G_c/G} - m_{\text{G}}[\Phi_\rho]\boldsymbol{v} \end{aligned} \tag{45}$$

General Body Rotational Equations of Motion

The general body rotational equations of motion are developed using Euler's equation

$$\dot{\boldsymbol{H}}_{\mathrm{G},G} = \sum \boldsymbol{L}_G - m_{\mathrm{G}}[\tilde{\boldsymbol{r}}_{G_c/G}]\ddot{\boldsymbol{r}}_{G/N} \tag{46}$$

where

$$\boldsymbol{H}_{\mathrm{G},G} = [I_{\mathrm{G},G}]\boldsymbol{\omega}_{\mathcal{G}/\mathcal{N}} \tag{47}$$

Taking the inertial time derivative of Eq. (47) gives the left-hand side of Eq. (46):

$$\begin{aligned}\dot{\boldsymbol{H}}_{\mathrm{G},G} = &\left[\widetilde{[\Phi_\theta][\boldsymbol{T}]\dot{\boldsymbol{\beta}} + \boldsymbol{\omega}_{\mathcal{B}/\mathcal{N}}}\right][I_{\mathrm{G},G}]\left([\Phi_\theta][\boldsymbol{T}]\dot{\boldsymbol{\beta}} + \boldsymbol{\omega}_{\mathcal{B}/\mathcal{N}}\right)\\ &+ [I_{\mathrm{G},G}][\Phi_\theta][\boldsymbol{T}]\ddot{\boldsymbol{\beta}} + [I_{\mathrm{G},G}][\Phi_\theta][\boldsymbol{T}']\dot{\boldsymbol{\beta}}\\ &+ [I_{\mathrm{G},G}][\tilde{\boldsymbol{\omega}}_{\mathcal{B}/\mathcal{N}}][\Phi_\theta][\boldsymbol{T}]\dot{\boldsymbol{\beta}} + [I_{\mathrm{G},G}]\dot{\boldsymbol{\omega}}_{\mathcal{B}/\mathcal{N}}\end{aligned} \tag{48}$$

Substitution of Eq. (48) into Eq. (46) and expanding $\ddot{\boldsymbol{r}}_{G/N}$ gives the general body rotational equations of motion

$$\begin{aligned}&\left([I_{\mathrm{G},G}][\Phi_\theta][\boldsymbol{T}] + m_{\mathrm{G}}[\tilde{\boldsymbol{r}}_{G_c/G}][\Phi_\rho]\left([\boldsymbol{T}] + [\boldsymbol{U}]\right)\right)\ddot{\boldsymbol{\beta}} = -m_{\mathrm{G}}[\tilde{\boldsymbol{r}}_{G_c/G}]\ddot{\boldsymbol{r}}_{B/N}\\ &-\left([I_{\mathrm{G},G}] - m_{\mathrm{G}}[\tilde{\boldsymbol{r}}_{G_c/G}]\left[\widetilde{[\Phi_\rho][\boldsymbol{T}]\boldsymbol{\beta}}\right]\right)\dot{\boldsymbol{\omega}}_{\mathcal{B}/\mathcal{N}}\\ &+\sum \boldsymbol{L}_G - \left[\widetilde{[\Phi_\theta][\boldsymbol{T}]\dot{\boldsymbol{\beta}} + \boldsymbol{\omega}_{\mathcal{B}/\mathcal{N}}}\right][I_{\mathrm{G},G}]\left([\Phi_\theta][\boldsymbol{T}]\dot{\boldsymbol{\beta}} + \boldsymbol{\omega}_{\mathcal{B}/\mathcal{N}}\right)\\ &-[I_{\mathrm{G},G}][\Phi_\theta][\boldsymbol{T}']\dot{\boldsymbol{\beta}} - [I_{\mathrm{G},G}][\tilde{\boldsymbol{\omega}}_{\mathcal{B}/\mathcal{N}}][\Phi_\theta][\boldsymbol{T}]\dot{\boldsymbol{\beta}}\\ &-m_{\mathrm{G}}[\tilde{\boldsymbol{r}}_{G_c/G}]\left([\Phi_\rho]\left(2[\boldsymbol{T}']\dot{\boldsymbol{\beta}} + \boldsymbol{v}\right) + 2[\tilde{\boldsymbol{\omega}}_{\mathcal{B}/\mathcal{N}}][\Phi_\rho]\left([\boldsymbol{T}]\dot{\boldsymbol{\beta}} + [\boldsymbol{T}']\boldsymbol{\beta}\right) + [\tilde{\boldsymbol{\omega}}_{\mathcal{B}/\mathcal{N}}]^2[\Phi_\rho][\boldsymbol{T}]\boldsymbol{\beta}\right)\end{aligned} \tag{49}$$

BACKSUBSTITUTION FORMULATION

Next, the general body equations of motion must be organized to facilitate integration with the hub equations of motion. Combining the general body equations yields

$$\underbrace{[\boldsymbol{M}_\beta]}_{6\times N}\ddot{\boldsymbol{\beta}} = \underbrace{[\boldsymbol{A}^*_\beta]}_{6\times 3}\ddot{\boldsymbol{r}}_{B/N} + \underbrace{[\boldsymbol{B}^*_\beta]}_{6\times 3}\dot{\boldsymbol{\omega}}_{\mathcal{B}/\mathcal{N}} + \underbrace{[\boldsymbol{C}^*_\beta]}_{6\times 1} \tag{50}$$

where

$$[\boldsymbol{M}_\beta] = \begin{bmatrix} m_{\mathrm{G}}\left(\left([\Phi_\rho] - \left[\tilde{\boldsymbol{r}}_{G_c/G}\right][\Phi_\theta]\right)[\boldsymbol{T}] + [\Phi_\rho][\boldsymbol{U}]\right)\\ [I_{\mathrm{G},G}][\Phi_\theta][\boldsymbol{T}] + m_{\mathrm{G}}[\tilde{\boldsymbol{r}}_{G_c/G}][\Phi_\rho]\left([\boldsymbol{T}] + [\boldsymbol{U}]\right)\end{bmatrix} \tag{51}$$

$$[\boldsymbol{A}^*_\beta] = \begin{bmatrix} -m_{\mathrm{G}}[I_{3\times 3}]\\ -m_{\mathrm{G}}[\tilde{\boldsymbol{r}}_{G_c/G}]\end{bmatrix} \tag{52}$$

$$[\boldsymbol{B}^*_\beta] = \begin{bmatrix} m_{\mathrm{G}}\left[\widetilde{\boldsymbol{r}_{G_c/G} + [\Phi_\rho][\boldsymbol{T}]\boldsymbol{\beta}}\right]\\ -\left([I_{\mathrm{G},G}] - m_{\mathrm{G}}[\tilde{\boldsymbol{r}}_{G_c/G}]\left[\widetilde{[\Phi_\rho][\boldsymbol{T}]\boldsymbol{\beta}}\right]\right)\end{bmatrix} \tag{53}$$

$$
[\boldsymbol{C}^*_\beta] = \begin{bmatrix} \sum \boldsymbol{F}_{\text{G}} - 2m_{\text{G}}[\tilde{\boldsymbol{\omega}}_{\mathcal{B}/\mathcal{N}}]\Big(\left([\Phi_\rho] - \left[\tilde{\boldsymbol{r}}_{G_c/G}\right][\Phi_\theta]\right)[\boldsymbol{T}]\dot{\boldsymbol{\beta}} + [\Phi_\theta][\boldsymbol{T}']\boldsymbol{\beta}\Big) \\ -m_{\text{G}}[\tilde{\boldsymbol{\omega}}_{\mathcal{B}/\mathcal{N}}]^2\left(\boldsymbol{r}_{G_c/G} + [\Phi_\rho][\boldsymbol{T}]\boldsymbol{\beta}\right) - m_{\text{G}}\left(2[\Phi_\rho] - \left[\tilde{\boldsymbol{r}}_{G_c/G}\right][\Phi_\theta]\right)[\boldsymbol{T}']\dot{\boldsymbol{\beta}} \\ -m_{\text{G}}\left[\widetilde{[\Phi_\theta][\boldsymbol{T}]\dot{\boldsymbol{\beta}}}\right]^2\boldsymbol{r}_{G_c/G} - m_{\text{G}}[\Phi_\rho]\boldsymbol{v} \\ \\ \sum \boldsymbol{L}_G - \left[\widetilde{[\Phi_\theta][\boldsymbol{T}]\dot{\boldsymbol{\beta}} + \boldsymbol{\omega}_{\mathcal{B}/\mathcal{N}}}\right][I_{\text{G},G}]\Big([\Phi_\theta][\boldsymbol{T}]\dot{\boldsymbol{\beta}} + \boldsymbol{\omega}_{\mathcal{B}/\mathcal{N}}\Big) \\ -[I_{\text{G},G}][\Phi_\theta][\boldsymbol{T}']\dot{\boldsymbol{\beta}} - [I_{\text{G},G}][\tilde{\boldsymbol{\omega}}_{\mathcal{B}/\mathcal{N}}][\Phi_\theta][\boldsymbol{T}]\dot{\boldsymbol{\beta}} \\ -m_{\text{G}}[\tilde{\boldsymbol{r}}_{G_c/G}]\Big([\Phi_\rho]\Big(2[\boldsymbol{T}']\dot{\boldsymbol{\beta}} + \boldsymbol{v}\Big) + 2[\tilde{\boldsymbol{\omega}}_{\mathcal{B}/\mathcal{N}}][\Phi_\rho]\Big([\boldsymbol{T}]\dot{\boldsymbol{\beta}} + [\boldsymbol{T}']\boldsymbol{\beta}\Big) + [\tilde{\boldsymbol{\omega}}_{\mathcal{B}/\mathcal{N}}]^2[\Phi_\rho][\boldsymbol{T}]\boldsymbol{\beta}\Big) \end{bmatrix} \tag{54}
$$

Next, Eq. 50 is rewritten as

$$
\ddot{\boldsymbol{\beta}} = [\boldsymbol{A}_\beta]\ddot{\boldsymbol{r}}_{B/N} + [\boldsymbol{B}_\beta]\dot{\boldsymbol{\omega}}_{\mathcal{B}/\mathcal{N}} + [\boldsymbol{C}_\beta] \tag{55}
$$

where

$$
[\boldsymbol{A}_\beta] = \left([\boldsymbol{T}]^T[\boldsymbol{M}_\beta]\right)^{-1}[\boldsymbol{T}]^T[\boldsymbol{A}^*_\beta] \tag{56}
$$

$$
[\boldsymbol{B}_\beta] = \left([\boldsymbol{T}]^T[\boldsymbol{M}_\beta]\right)^{-1}[\boldsymbol{T}]^T[\boldsymbol{B}^*_\beta] \tag{57}
$$

$$
[\boldsymbol{C}_\beta] = \left([\boldsymbol{T}]^T[\boldsymbol{M}_\beta]\right)^{-1}[\boldsymbol{T}]^T[\boldsymbol{C}^*_\beta] \tag{58}
$$

Back-substituting these results into the system equations of motion given by Eqs. (32) and (42) yields the final form of the system equations of motion

$$
\begin{bmatrix} [A] & [B] \\ [C] & [D] \end{bmatrix}\begin{bmatrix} \ddot{\boldsymbol{r}}_{B/N} \\ \dot{\boldsymbol{\omega}}_{\mathcal{B}/\mathcal{N}} \end{bmatrix} = \begin{bmatrix} \boldsymbol{v}_{\text{trans}} \\ \boldsymbol{v}_{\text{rot}} \end{bmatrix} \tag{59}
$$

The matrices are defined as

$$
[A] = m_{\text{sc}}[I_{3\times 3}] + m_{\text{G}}\left(\left([\Phi_\rho] - \left[\tilde{\boldsymbol{r}}_{G_c/G}\right][\Phi_\theta]\right)[\boldsymbol{T}] + [\Phi_\rho][\boldsymbol{U}]\right)[\boldsymbol{A}_\beta] \tag{60}
$$

$$
[B] = -m_{\text{sc}}[\tilde{\boldsymbol{c}}] + m_{\text{G}}\left(\left([\Phi_\rho] - \left[\tilde{\boldsymbol{r}}_{G_c/G}\right][\Phi_\theta]\right)[\boldsymbol{T}] + [\Phi_\rho][\boldsymbol{U}]\right)[\boldsymbol{B}_\beta] \tag{61}
$$

$$
\begin{aligned} [C] &= m_{\text{sc}}[\tilde{\boldsymbol{c}}] \\ &\quad + \Big([I_{\text{G},G_c}][\Phi_\theta][\boldsymbol{T}] + m_{\text{G}}\left[\widetilde{\boldsymbol{r}_{G_c/G} + [\Phi_\rho]}[\boldsymbol{T}]\boldsymbol{\beta}\right]\left(\left([\Phi_\rho] - \left[\tilde{\boldsymbol{r}}_{G_c/G}\right][\Phi_\theta]\right)[\boldsymbol{T}] + [\Phi_\rho][\boldsymbol{U}]\right)\Big)[\boldsymbol{A}_\beta] \end{aligned} \tag{62}
$$

$$
\begin{aligned} [D] &= [I_{\text{sc},B}] \\ &\quad + \Big([I_{\text{G},G_c}][\Phi_\theta][\boldsymbol{T}] + m_{\text{G}}\left[\widetilde{\boldsymbol{r}_{G_c/G} + [\Phi_\rho]}[\boldsymbol{T}]\boldsymbol{\beta}\right]\left(\left([\Phi_\rho] - \left[\tilde{\boldsymbol{r}}_{G_c/G}\right][\Phi_\theta]\right)[\boldsymbol{T}] + [\Phi_\rho][\boldsymbol{U}]\right)\Big)[\boldsymbol{B}_\beta] \end{aligned} \tag{63}
$$

The vector components group the remaining terms

$$
\begin{aligned} \boldsymbol{v}_{\text{trans}} = \sum \boldsymbol{F}_{\text{ext}} &- 2m_{\text{sc}}[\tilde{\boldsymbol{\omega}}_{\mathcal{B}/\mathcal{N}}]\boldsymbol{c}' - m_{\text{sc}}[\tilde{\boldsymbol{\omega}}_{\mathcal{B}/\mathcal{N}}]^2\boldsymbol{c} \\ &- m_{\text{G}}\left(2[\Phi_\rho] - \left[\tilde{\boldsymbol{r}}_{G_c/G}\right][\Phi_\theta]\right)[\boldsymbol{T}']\dot{\boldsymbol{\beta}} \\ &- m_{\text{G}}\left[\widetilde{[\Phi_\theta][\boldsymbol{T}]\dot{\boldsymbol{\beta}}}\right]^2\boldsymbol{r}_{G_c/G} - m_{\text{G}}[\Phi_\rho]\boldsymbol{v} \end{aligned}
$$

$$
- m_{\mathrm{G}} \left(\left([\Phi_\rho] - \left[\tilde{\boldsymbol{r}}_{G_c/G} \right] [\Phi_\theta] \right) [\boldsymbol{T}] + [\Phi_\rho][\boldsymbol{U}] \right) [\boldsymbol{C}_\beta] \tag{64}
$$

$$
\begin{aligned}
\boldsymbol{v}_{\mathrm{rot}} = & \sum \boldsymbol{L}_B - \left([I'_{\mathrm{sc},B}] + [\tilde{\boldsymbol{\omega}}_{\mathcal{B}/\mathcal{N}}][I_{\mathrm{sc},B}] \right) \boldsymbol{\omega}_{\mathcal{B}/\mathcal{N}} \\
& - [I_{\mathrm{G},G_c}][\Phi_\theta][\boldsymbol{T}']\dot{\boldsymbol{\beta}} - \left[\widetilde{[\Phi_\theta][\boldsymbol{T}]\dot{\boldsymbol{\beta}} + \boldsymbol{\omega}_{\mathcal{B}/\mathcal{N}}} \right] [I_{\mathrm{G},G_c}][\Phi_\theta][\boldsymbol{T}]\dot{\boldsymbol{\beta}} \\
& - m_{\mathrm{G}} \left[\widetilde{\boldsymbol{r}_{G_c/G} + [\Phi_\rho][\boldsymbol{T}]\boldsymbol{\beta}} \right] \left(\left(2[\Phi_\rho] - \left[\tilde{\boldsymbol{r}}_{G_c/G} \right] [\Phi_\theta] \right) [\boldsymbol{T}']\dot{\boldsymbol{\beta}} + \left[\widetilde{[\Phi_\theta][\boldsymbol{T}]\dot{\boldsymbol{\beta}}} \right]^2 \boldsymbol{r}_{G_c/G} + [\Phi_\rho]\boldsymbol{v} \right) \\
& - m_{\mathrm{G}}[\tilde{\boldsymbol{\omega}}_{\mathcal{B}/\mathcal{N}}] \left[\widetilde{\boldsymbol{r}_{G_c/G} + [\Phi_\rho][\boldsymbol{T}]\boldsymbol{\beta}} \right] \left(\left([\Phi_\rho] - \left[\tilde{\boldsymbol{r}}_{G_c/G} \right] [\Phi_\theta] \right) [\boldsymbol{T}]\dot{\boldsymbol{\beta}} + [\Phi_\rho][\boldsymbol{T}']\boldsymbol{\beta} \right) \\
& - \left([I_{\mathrm{G},G_c}][\Phi_\theta][\boldsymbol{T}] + m_{\mathrm{G}} \left[\widetilde{\boldsymbol{r}_{G_c/G} + [\Phi_\rho][\boldsymbol{T}]\boldsymbol{\beta}} \right] \left(\left([\Phi_\rho] - \left[\tilde{\boldsymbol{r}}_{G_c/G} \right] [\Phi_\theta] \right) [\boldsymbol{T}] + [\Phi_\rho][\boldsymbol{U}] \right) \right) [\boldsymbol{C}_\beta]
\end{aligned} \tag{65}
$$

NUMERICAL SIMULATION

This section presents a spacecraft multi-body deployment simulation scenario utilizing the general effector developed in this work. The scenario demonstrates the benefit of the general effector solution, where two distinct types of rigid body motion are configured using the same general formulation. The general equations of motion are implemented in the open-source Basilisk simulation framework[‡], which uses the backsubstitution method[25] for the spacecraft dynamics formulation.

The spacecraft design and deployment dynamics chosen for this scenario are modeled after the IXPE spacecraft[40,41] due to its unique deployment sequence. Illustrated in Fig. (2), the spacecraft system consists of four rigid bodies, three of which are modeled using the general effector formulation. The three general components are attached to a 150 kg rigid cubic hub (gray). Two single degree-of-freedom 1×1 meter 10 kg solar panels (blue) rotate relative to the central hub during deployment, while a 170 kg single degree-of-freedom cylindrical payload (orange) follows coupled translational and rotational screw motion relative to the hub during deployment. Starting from rest in the stowed configurations seen in Fig. 2(a), the solar panels are first deployed by 90 degrees in two minutes to the configuration seen in Fig. 2(b). After the solar panel motion dampens, the payload is deployed 3 meters along the hub's third axis in three minutes while completing 3.5 revolutions about the same axis. The general body deployments are commanded using rotational spring-dampers which track the reference motion profiles. Tables 2, 3 and 4 provide additional parameters and relevant mass properties for the system components.

The simulated component displacements and rates are provided in Fig. (3). The solar panel angles and rates are shown in Figs. 3(a) and 3(b), while the payload displacements and rates are shown in Figs. 3(c) and 3(d). As expected, the solar panels deploy during the first two minutes of the simulation, followed by deployment of the payload during the final three minutes of the simulation. The component reference profiles are simulated using smoothed bang-bang acceleration profiles.[31]

The hub's response to the deployment motion is illustrated in Fig. (4). Figure 4(a) provides the hub inertial attitude expressed in Modified Rodriguez Parameters,[?] while Figs. 4(b) and 4(c) show the hub inertial angular velocity and inertial position, respectively. Because the system starts from

[‡] `https://avslab.github.io/basilisk`

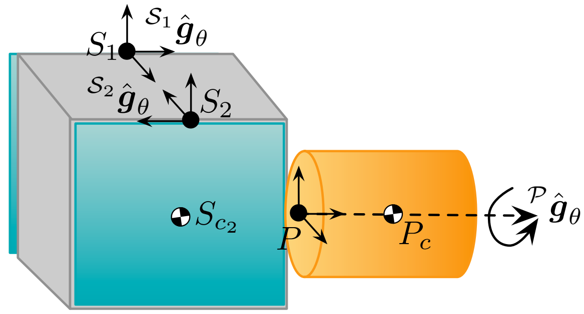

(a) Stowed configuration.

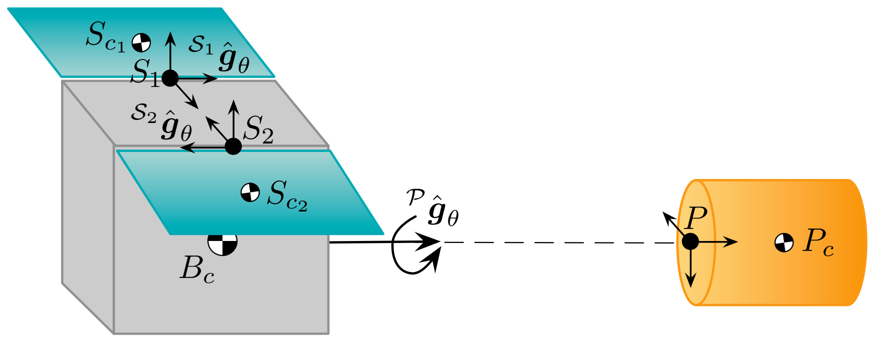

(b) Deployed configuration.

Figure 2. Spacecraft stowed and deployed configurations.

rest, the induced hub motion is purely due to the dynamic coupling between all of the system components. The hub is seen to move in opposition to the component deployments, which is required to conserve the system angular momentum. The bulk of the hub motion is observed during the payload deployment, as it must compensate for the large three meter translation and 1260 degree rotation of the payload. As expected, the hub returns to a state of rest after the deployment is complete.

CONCLUSION

This paper presents a novel new generalized backsubstitution formulation for simulating any type of six-degree-of-freedom rigid body motion using a joint mapping approach. The final formulation is implemented modularly and verified in the Basilisk astrodynamics simulation software. The modular dynamics implementation enables a spacecraft system to be easily scaled to N general component attachments to the central hub structure. The scalability and versatility of the general formulation is demonstrated using a numerical spacecraft system deployment example, where three general components are commanded to actuate relative to a central rigid hub during the system deployment.

REFERENCES

[1] M. J. Sidi, *Spacecraft Dynamics and Control: A Practical Engineering Approach*, Vol. 7. Cambridge University Press, 1997.

[2] H. Schaub and J. L. Junkins, *Analytical Mechanics of Space Systems*. Reston, Virginia: American Institute of Aeronautics and Astronautics, Inc., 5 ed., 2018.

[3] W. W. Hooker, "A Set of r Dynamical Attitude Equations for an Arbitrary n-Body Satellite Having r Rotational Degrees of Freedom," *AIAA Journal*, Vol. 8, No. 7, 1970, pp. 1205–1207, 10.2514/3.5873.

Table 2. Hub simulation parameters.

Parameter	Notation	Value	Unit
Hub mass	m_{hub}	150	kg
Hub inertia about its center of mas	${}^{\mathcal{B}}[I_{\text{hub},B_c}]$	$\begin{bmatrix} 21.67 & 0 & 0 \\ 0 & 21.67 & 0 \\ 0 & 0 & 21.67 \end{bmatrix}$	kg $\cdot$ m^2
Hub center of mass location with respect to point B	${}^{\mathcal{B}}\boldsymbol{r}_{B_c/B}$	[0, 0, 0]	m
Hub initial inertial angular velocity	${}^{\mathcal{B}}\boldsymbol{\omega}_{\mathcal{B}/\mathcal{N}}$	[0, 0, 0]	rad / s

Table 3. Solar panel parameters.

Parameter	Notation	Value	Unit
Panel mass	m_{S}	10	kg
Panel inertia about its center of mass	${}^{\mathcal{S}}[I_{\text{S},S_c}]$	$\begin{bmatrix} 0.8334 & 0 & 0 \\ 0 & 1.6667 & 0 \\ 0 & 0 & 0.8334 \end{bmatrix}$	kg $\cdot$ m^2
Panel frame locations with respect to point B	${}^{\mathcal{B}}\boldsymbol{r}_{S/B}$	[$\pm$ 0.5, 0, 0]	m
Panel center of mass locations with respect to point S	${}^{\mathcal{S}}\boldsymbol{r}_{S_c/S}$	[$\pm$ 0.5, 0, 0]	m
Panel bending rotation axes	${}^{\mathcal{S}}\hat{\boldsymbol{g}}_{\theta}$	[1, 0, 0]	—
Rotational spring constant	k	$7 \cdot 10^5$	N $\cdot$ m / rad
Rotational damper constant	c	$5 \cdot 10^4$	N $\cdot$ m $\cdot$ s / rad

Table 4. Payload parameters.

Parameter	Notation	Value	Unit
Payload mass	m_{P}	170	kg
Payload inertia about its center of mass	${}^{\mathcal{P}}[I_{\mathrm{P},P_c}]$	$\begin{bmatrix} 24.79 & 0 & 0 \\ 0 & 24.79 & 0 \\ 0 & 0 & 21.25 \end{bmatrix}$	$\mathrm{kg} \cdot \mathrm{m}^2$
Payload initial location with respect to point B	${}^{\mathcal{B}}\boldsymbol{r}_{P_0/B}$	[0, 0, 0.5]	m
Payload deployed location with respect to point B	${}^{\mathcal{B}}\boldsymbol{r}_{P/B}$	[0, 0, 3.5]	m
Payload center of mass location with respect to point P	${}^{\mathcal{P}}\boldsymbol{r}_{P_c/P}$	[0, 0, 0.5]	m
Payload rotation/translation axis	${}^{\mathcal{P}}\hat{\boldsymbol{g}}_{\theta}$	[0, 0, 1]	—
Rotational spring constant	k	$7 \cdot 10^5$	N · m / rad
Rotational damper constant	c	$5 \cdot 10^4$	N · m · s / rad

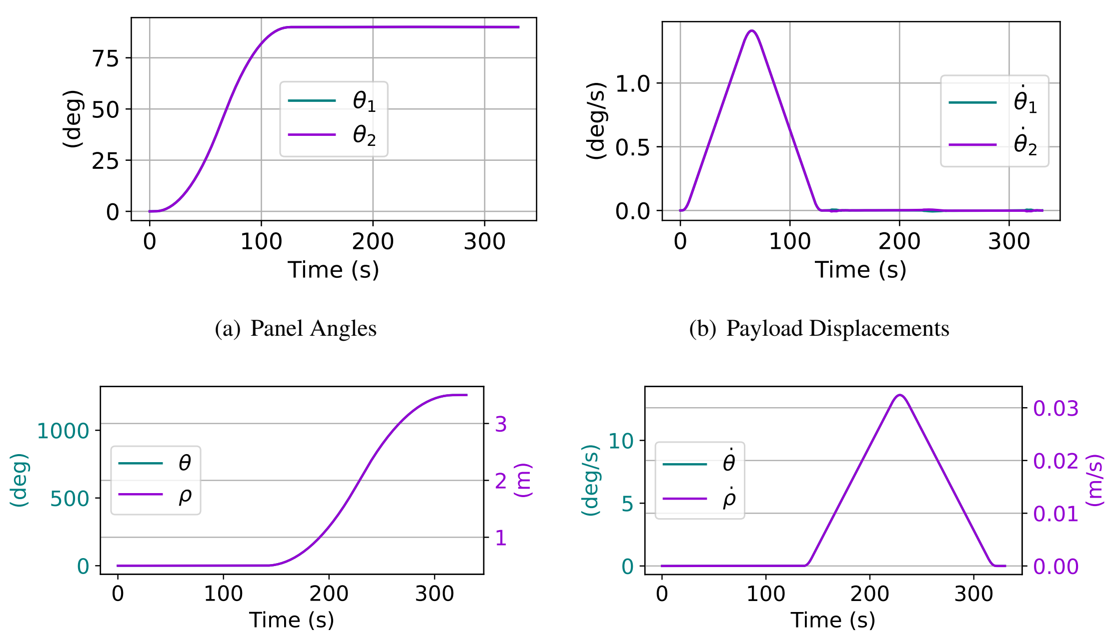

(a) Panel Angles

(b) Payload Displacements

(c) Panel Rates

(d) Payload Rates

Figure 3. Component Displacements and Rates.

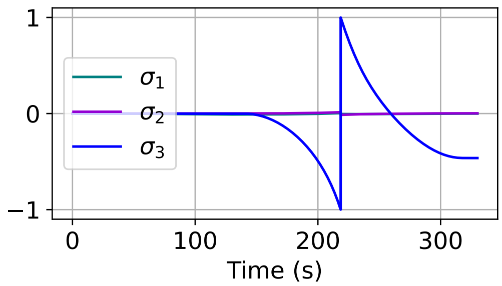

(a) Hub inertial attitude $\boldsymbol{\sigma}_{\mathcal{B}/\mathcal{N}}$.

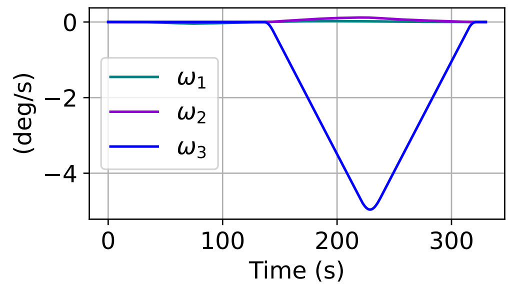

(b) Hub inertial angular velocity ${}^{\mathcal{B}}\boldsymbol{\omega}_{B/N}$.

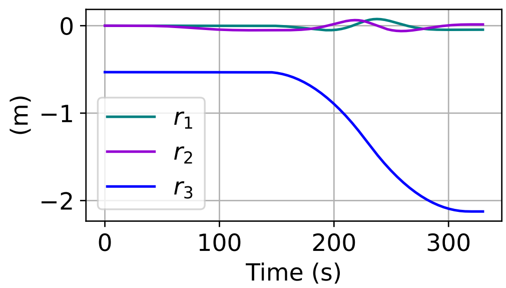

(c) Hub inertial position ${}^{\mathcal{N}}\boldsymbol{r}_{B/N}$.

Figure 4. Hub response.

[4] V. J. Modi, "Attitude Dynamics of Satellites with Flexible Appendages—A Brief Review," *Journal of Spacecraft and Rockets*, Vol. 11, No. 11, 1974, pp. 743–751, 10.2514/3.62172.

[5] P. W. Likins, "Point-connected Rigid Bodies in a Topological Tree," *Celestial Mechanics*, Vol. 11, No. 3, 1975, pp. 301–317, 10.1007/BF01228809.

[6] B. Paul, "Analytical dynamics of mechanisms—a computer oriented overview," *Mechanism and Machine Theory*, Vol. 10, No. 6, 1975, pp. 481–507, 10.1016/0094-114X(75)90005-1.

[7] W. Jerkovsky, "The Structure of Multibody Dynamics Equations," *Journal of Guidance and Control*, Vol. 1, No. 3, 1978, pp. 173–182, 10.2514/3.55761.

[8] J. Y. S. Luh, M. W. Walker, and R. P. C. Paul, "On-Line Computational Scheme for Mechanical Manipulators," *Journal of Dynamic Systems, Measurement, and Control*, Vol. 102, June 1980, pp. 69–76, 10.1115/1.3149599.

[9] M. W. Walker and D. E. Orin, "Efficient Dynamic Computer Simulation of Robotic Mechanisms," *Journal of Dynamic Systems, Measurement, and Control*, Vol. 104, Sept. 1982, pp. 205–211, 10.1115/1.3139699.

[10] A. Jain, "Unified Formulation of Dynamics for Serial Rigid Multibody System," *Journal of Guidance, Control, and Dynamics*, Vol. 14, No. 3, 1991, pp. 531–542, 10.2514/3.20672.

[11] K. Anderson, "An Order N Formulation for the Motion Simulation of General Multi-Rigid-Body Tree Systems," *Computers & Structures*, Vol. 46, No. 3, 1993, pp. 547–559, 10.1016/0045-7949(93)90224-2.

[12] S. Pradhan, V. J. Modi, and A. K. Misra, "Order N Formulation for Flexible Multibody Systems in Tree Topology: Lagrangian Approach," *Journal of Guidance, Control, and Dynamics*, Vol. 20, No. 4, 1997, pp. 665–672, 10.2514/2.4129.

[13] A. K. Banerjee, "Contributions of Multibody Dynamics to Space Flight: A Brief Review," *Journal of Guidance, Control, and Dynamics*, Vol. 26, No. 3, 2003, pp. 385–394, 10.2514/2.5069.

[14] J. Critchley and K. S. Anderson, "A Generalized Recursive Coordinate Reduction Method for Multibody System Dynamics," *International Journal for Multiscale Computational Engineering*, Vol. 1, No. 2&3, 2003, 10.1615/IntJMultCompEng.v1.i23.50.

[15] R. Featherstone, *Rigid Body Dynamics Algorithms*. Springer New York, 2008, 10.1007/978-1-4899-7560-7.

[16] R. Featherstone, "The Calculation of Robot Dynamics Using Articulated-Body Inertias," *The International Journal of Robotics Research*, Vol. 2, No. 1, 1983, pp. 13–30, 10.1177/027836498300200102.

[17] R. Featherstone, *Robot Dynamics Algorithms*. Springer New York, NY, 1987, 10.1007/978-0-387-74315-8.

[18] M. Brady, J. M. Hollerbach, T. L. Johnson, T. Lozano-Pérez, and M. T. Mason, eds., *Robot Motion: Planning and Control*. Cambridge, MA: The MIT Press, 1982.

[19] G. Rodriguez, A. Jain, and K. Kreutz-Delgado, "A Spatial Operator Algebra for Manipulator Modeling and Control," *The International Journal of Robotics Research*, Vol. 10, No. 4, 1991, pp. 371–381, 10.1177/027836499101000406.

[20] A. Jain and G. Rodriguez, "Recursive Flexible Multibody Dynamics Using Spatial Operators," Vol. 16, 1993, pp. 345–358, 10.1016/B978-0-444-89856-2.50036-3.

[21] A. Jain, *Robot and Multibody Dynamics: Analysis and Algorithms*. Springer Science & Business Media, 2010.

[22] C. Allard, M. D. Ramos, H. Schaub, P. Kenneally, and S. Piggott, "Modular Software Architecture for Fully Coupled Spacecraft Simulations," *Journal of Aerospace Information Systems*, Vol. 15, No. 12, 2018, pp. 670–683.

[23] P. W. Kenneally, S. Piggott, and H. Schaub, "Basilisk: A Flexible, Scalable and Modular Astrodynamics Simulation Framework," *Journal of Aerospace Information Systems*, Vol. 17, Sept. 2020, pp. 496–507.

[24] C. Allard, M. D. Ramos, and H. Schaub, "Computational Performance of Complex Spacecraft Simulations Using Back-Substitution," *Journal of Aerospace Information Systems*, Vol. 16, No. 10, 2019, pp. 427–436.

[25] J. Vaz Carneiro and H. Schaub, "Spacecraft Dynamics With The Backsubstitution Method: Survey And Capabilities," *AAS Spaceflight Mechanics Meeting*, Kauai, Hawaii, Jan. 19–23 2025. Paper No. AAS 25-232.

[26] C. Allard, H. Schaub, and S. Piggott, "General Hinged Rigid-Body Dynamics Approximating First-Order Spacecraft Solar Panel Flexing," *Journal of Spacecraft and Rockets*, Vol. 55, No. 5, 2018, pp. 1290–1298.

[27] J. Alcorn, C. Allard, and H. Schaub, "Fully Coupled Reaction Wheel Static and Dynamic Imbalance for Spacecraft Jitter Modeling," *AIAA Journal of Guidance, Control, and Dynamics*, Vol. 41, No. 6, 2018, pp. 1380–1388, 10.2514/1.G003277.

[28] J. Alcorn, C. Allard, and H. Schaub, "Fully-Coupled Dynamical Jitter Modeling Of Variable-Speed Control Moment Gyroscopes," *AAS/AIAA Astrodynamics Specialist Conference*, Stevenson, WA, Aug. 20–24 2017. Paper No. AAS-17-730.

[29] C. Allard, M. Diaz-Ramos, and H. Schaub, "Spacecraft Dynamics Integrating Hinged Solar Panels and Lumped-Mass Fuel Slosh Model," *AIAA/AAS Astrodynamics Specialist Conference*, Long Beach, CA, Sept. 12–15 2016.

[30] P. Cappuccio, C. Allard, and H. Schaub, "Fully-Coupled Spherical Modular Pendulum Model To Simulate Spacecraft Propellant Slosh," *AAS/AIAA Astrodynamics Specialist Conference*, Snowbird, UT, August 19–23 2018. Paper No. AAS-18-224.

[31] L. Kiner, H. Schaub, and C. Allard, "Spacecraft Backsubstitution Dynamics with General Multibody Prescribed Subcomponents," *Journal of Aerospace Information Systems*, Vol. 22, August 2025, pp. 703–715, 10.2514/1.I011491.

[32] L. Kiner, C. Allard, and H. Schaub, "Two-Axis Gimbal Simulation Overview For The Emirates Mission To The Asteroid Belt," *AAS Guidance, Navigation and Control Conference*, Breckenridge, CO, Jan. 31 – Feb. 5 2025. Paper No. AAS-25-013.

[33] L. Kiner and H. Schaub, "Backsubstitution Method For Prescribed Motion Actuators With Attached Dynamic Sub-Components," *AAS/AIAA Astrodynamics Specialist Conference*, Boston, MA, August 10–14 2025. Paper No. AAS 25-790.

[34] A. Morell and H. Schaub, "Back-Substitution Based Spacecraft Dynamics Modeling With Selective Configuration Space Branching," *AAS Astrodynamics Specialist Conference*, Broomfield, CO, Aug. 11–15 2024. Paper No. AAS 24-361.

[35] A. Morell and H. Schaub, "Expanded Backsubstitution Dynamics Modeling For Branched Force And Torque Based Spacecraft Components," *AAS Spaceflight Mechanics Meeting*, Kauai, Hawaii, Jan. 19–23 2025. Paper No. AAS 25-185.

[36] J. Vaz Carneiro, C. Allard, and H. Schaub, "General Dynamics for Single- and Dual-Axis Rotating Rigid Spacecraft Components," *Journal of Spacecraft and Rockets*, Vol. 61, July–August 2024, pp. 1099–1113, 10.2514/1.A35865.

[37] J. Vaz Carneiro, C. Allard, and H. Schaub, "Effector Dynamics For Sequentially Rotating Rigid Body Spacecraft Components," *AAS/AIAA Astrodynamics Specialist Conference*, Big Sky, MO, Aug. 13–17 2023. Paper AAS 23–192.

[38] J. Vaz Carneiro, P. Johnson, and H. Schaub, "Backsubstitution Method For Spacecraft With Generally Translating Appendages," *AAS Astrodynamics Specialist Conference*, Broomfield, CO, Aug. 11–15 2024. Paper No. AAS 24-248.

[39] C. Allard, J. Maxwell, and H. Schaub, "A Transport Theorem for the Inertia Tensor for Simplified Spacecraft Dynamics Development," *International Astronautical Congress*, Paris, France, Sept. 18–22 2022.

[40] eoPortal, "IXPE (Imaging X-ray Polarimetry Explorer)," `https://directory.eoportal.org/satellite-missions/ixpe#references`, 2017.

[41] IXPE Science Operations Center, "IXPE Science Operations Center User Guide — Observatory," User Guide ST-12, National Aeronautics and Space Administration, 2022.